Ballistic Range and Aerothermodynamic Testing

A. W. Strawa* and G. T. Chapman†
NASA Ames Research Center, Moffett Field, California 94035
T. N. Canning‡
Eloret Institute, Sunnyvale, California 94087
and
J. O. Arnold§
NASA Ames Research Center, Moffett Field, California 94035

Recent interest in hypervelocity vehicles requires an increase in our understanding of aerothermodynamic phenomena. Tests conducted in ground-based facilities will be used to better our understanding of the physics of hypervelocity flight and to verify computer models that will be used to predict vehicle performance in this environment. This paper reviews the requirements for aerothermodynamic testing and discusses the role of the aeroballistic range in accomplishing these requirements. Examples of the kinds of testing performed in typical high-performance aeroballistic ranges are described. Prospects for improving the capabilities of the aeroballistic range by using advanced instrumentation are discussed. Finally, recent developments in high-speed launch technology and their application to extend aeroballistic range capabilities are summarized.

Introduction

INTEREST in designing a variety of vehicles which fly at hypervelocities and at high altitudes is increasing. Recent studies, such as the Paine Commission Report,[1] have identified the need for reusable vehicles that aerobrake and aeromaneuver in support of the space station, lunar bases, and exploration of Mars. The Office of Space and Technology Planning has identified the need for enhanced hypersonic capability with air-breathing propulsion.[2] Programs under way in this nation include the Aeroassisted Flight Experiment (AFE)[3,4] and the National AeroSpace Plane (NASP).[5] The AFE (part of NASA's Civilian Space Technology Initiative) will test concepts for aerobraking in the upper atmosphere that will be used in the design of Aeroassisted Space Transfer Vehicles (ASTV). The NASP program is aimed at designing a horizontal takeoff and landing, single-stage-to-orbit vehicle. Both of these programs will increase our understanding of the phenomena involved with this class of vehicles and improve the nation's technology base. Similar programs are underway in other nations.

The flight environment of these future missions and of several past missions is shown in Fig. 1. The boundaries at which chemical and thermodynamic phenomena become important are also shown. It can be seen that the new missions expand the flight environment, which makes additional physical phenomena important and imposes additional aerothermodynamic requirements. Nearly all of the mission profiles occur where there are significant amounts of oxygen and nitrogen dissociation. The higher velocity missions (for example the Mars sample-return) also encounter significant amounts of ionization. The air-breathing NASP vehicle flies well beyond the region of our present experience and understanding of air-breathing propulsion, which is typified by the Concorde mission profile in the lower left corner of the chart. The lower boundary of the NASP flight envelope is the leg from takeoff to orbit, during which very high dynamic pressure is necessary to provide adequate oxygen for air-breathing propulsion. This results in very high Reynolds numbers and hence boundary-layer transition and turbulent flow, which causes high drag and heat transfer. ASTVs spend nearly their entire flight lives at very high altitudes and encounter significant amounts of chemical and thermodynamic nonequilibrium.

The design of these vehicles will require the coordinated use of ground based facilities, flight research, and computational fluid dynamics capabilities as the requirements for aerothermodynamic testing become more complex. Aerodynamic forces and moments, including the effects of control surfaces, must be known and understood. The various fluid dynamic and chemical processes that occur under the appropriate flight conditions must be included. Detailed knowledge of the heat transfer, convective as well as radiative, that these vehicles will experience under the extreme conditions of the various flight profiles is required. Of increasing importance are the special aerodynamic problems associated with the integration of the propulsion systems with the airframe for vehicles such as NASP. Here, not only the chemical processes of the external flow, but those associated with the power plant must be considered.

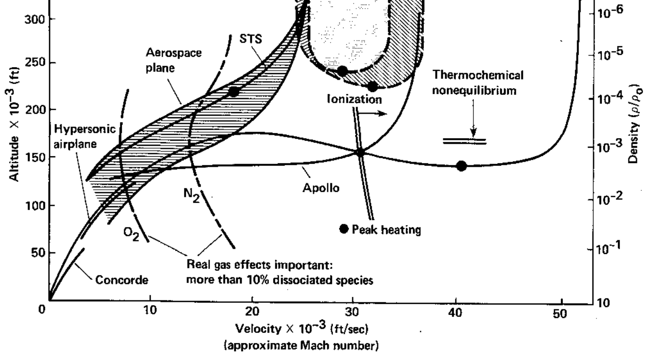

Fig. 1 Hypersonic flight environment.

Presented as Paper 88-2015 at the AIAA 15th Aerodynamic Testing Conference, San Diego, CA, May 18–20, 1988; received Oct. 7, 1989; revision received Aug. 20, 1990; accepted for publication Sept. 1, 1990.

*Research Scientist. Member AIAA.
†Senior Staff Scientist. Associate Fellow AIAA.
‡Senior Research Scientist.
§Division Chief, Thermodynamics Division.

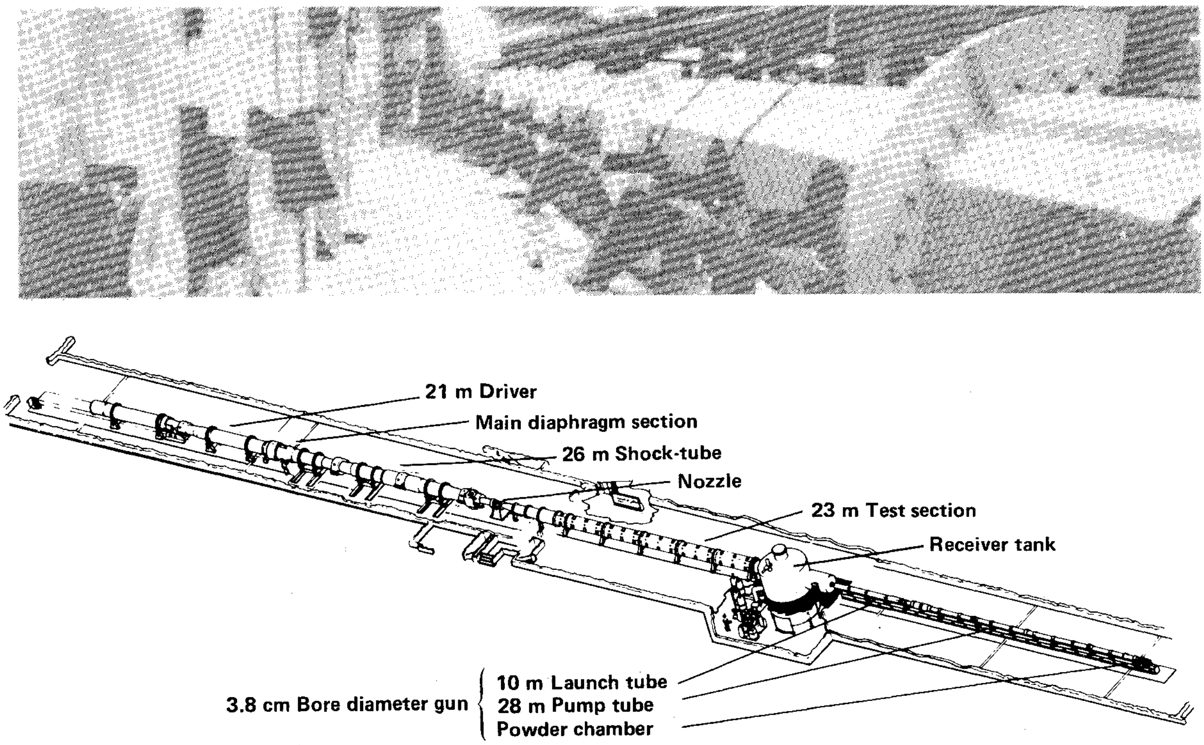

Fig. 2 NASA Ames Hypervelocity Free-Flight Aerodynamic Facility.

The items mentioned so far have been overall design-related issues, but their resolution will require detailed information about the basic phenomena that occur in these flight environments. The most significant physical phenomena are high temperature thermodynamic and chemical effects; boundary layer transition and turbulence; combustion for the air-breathing vehicles; and specific flow structures such as shock waves, shear layers, separated flows, vortical flows, wakes, and the interaction of these structures. Once the relevant phenomena have been understood, they must be incorporated into computational fluid dynamics (CFD) codes. Since ground-based facilities cannot fully simulate the environment in which future aerospace vehicles will fly, CFD and flight testing will be increasingly relied upon for vehicle design. The rapid development of CFD methodology and the large increase in computational capability that has become available in the last 10 years allow the solution of ever more complicated flows about complex shapes. However, the CFD codes must be verified by experiment before they can be used in vehicle design. CFD code verification requires dedicated experiments to be performed in our ground-based facilities. Also, design concepts must be tested with flight experiments.

Meeting all of these requirements with the presently available ground-based facilities will be difficult. The aeroballistic range has the ability to meet many of these requirements, and its unique capabilities are the subject of this paper. Examples of typical testing performed in high-performance aeroballistic ranges are described. Finally, we discuss improvements needed in our existing facilities to meet the aerothermodynamic requirements of the future. We draw heavily on experience obtained in the aeroballistic facilities at the NASA Ames Research Center.

Aeroballistic Range Characteristics

The discussion in this paper is concerned with aerothermodynamic testing in aeroballistic ranges at hypersonic conditions. Present high-performance aeroballistic ranges consist of a two-stage light-gas gun, which is used to launch the model, a tank in which to separate the sabot from the model and eliminate gun gases, and a test section where the major portion of the instrumentation is located. (The sabot is used to encase the model in the launch tube and to help support the model during the high acceleration loads experienced during launch. After launch the sabot pieces are separated from the model, usually by aerodynamic forces, and the model is free to travel through the test section.) A schematic of a typical aeroballistic facility, namely the Hypersonic Free-Flight Aerodynamic Facility (HFFAF) at NASA Ames, is shown in Fig. 2. The HFFAF also has a counterflow capability. A large shock tube (shown in Fig. 2) is used to generate a Mach 7 airflow through the test section in the opposite direction of model flight to increase the relative Mach number. A complete description of the HFFAF and aeroballistic range technology can be found in Ref. 6. The envelope of test conditions for the HFFAF is shown in Fig. 3 superimposed on some of the flight regimes of interest. This is very typical of other high-performance aeroballistic ranges. It can be seen that the aeroballistic range covers a significant portion of the missions shown. Maximum attainable velocity is presently about 9 km/s. A wide range of Mach and Reynolds numbers (M = 0.2 to 22, 30 with counterflow, and Re = 2.5×10^2 to 3×10^7) are possible. Freestream

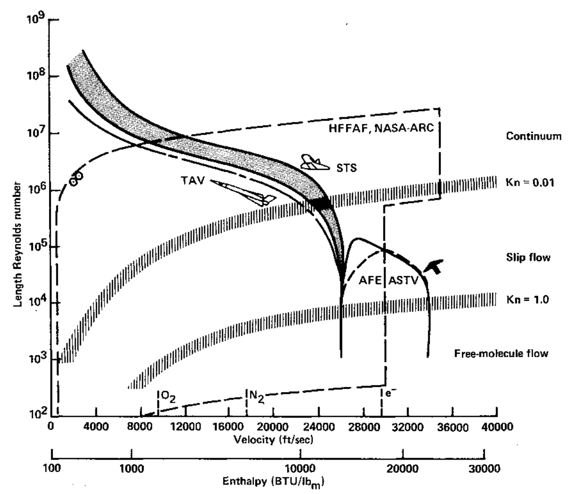

Fig. 3 Simulation capability of the HFFAF.

chemical conditions equivalent to flight are achieved, and there is very little freestream flow disturbance. The test gas can be readily changed to any other gas. A very wide assortment of models have been launched in aeroballistic facilities. Models launched at the Ames facility vary in size from 0.2 to 1.5 in. in diam and from a few milligrams to 50 g in mass. Configurations which exhibit lift may be launched but require special launch techniques.

Besides the facilities at NASA Ames, there are very few aeroballistic facilities in the nation suitable for aerothermodynamic testing at hypersonic velocities. Two of these are at the Arnold Engineering Development Center (AEDC) at the Arnold Air Force Station and the Air Force Armament Laboratory at Eglin Air Force Base. The AEDC facility can launch models up to 2.5 in. in diam and employs a track system for controlling the location of the model within the test section. The maximum velocity attainable in the Eglin facility is limited to about 4 km/s.

Although the aeroballistic range has a large simulation capability, data acquistion can be difficult. Most data acquisition must be done as the model flies past the measurement station. At hypervelocity this can mean a measurement time on the order of tens of nanoseconds. Since the model is in freeflight, its exact position at the measurement station is not known a priori, and most instruments require a wide field of view. At the present time, all data at high speed are acquired remotely, although some attempts to use onboard instrumentation have been made. Present gun technology requires that models be relatively small and simple. Models and sabots must be carefully designed since acceleration loads in the launch tube frequently exceed 500,000 *g*. Complex models can be flown, but they require gentle launches, and in most cases they

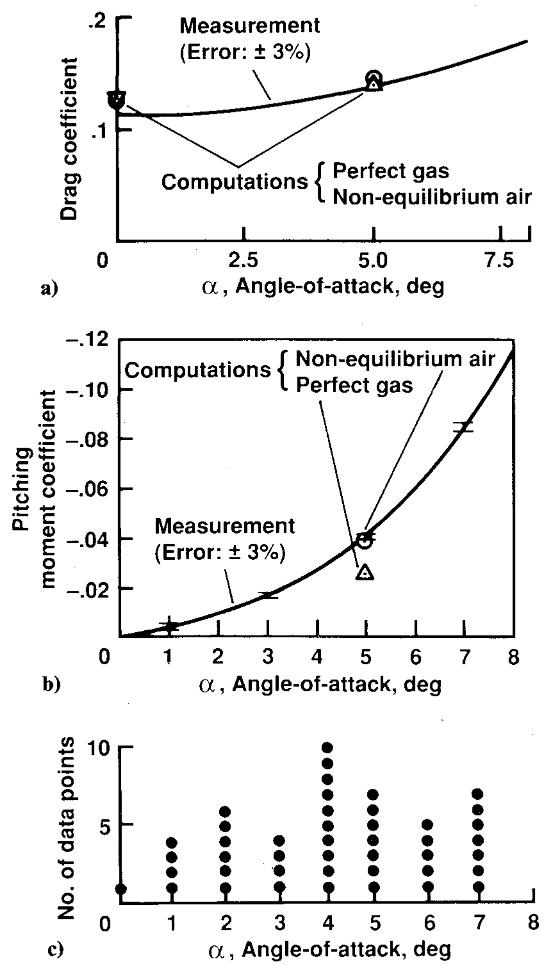

Fig. 4 Drag and pitching moment coefficients vs angle of attack for a blunt 5-deg cone.

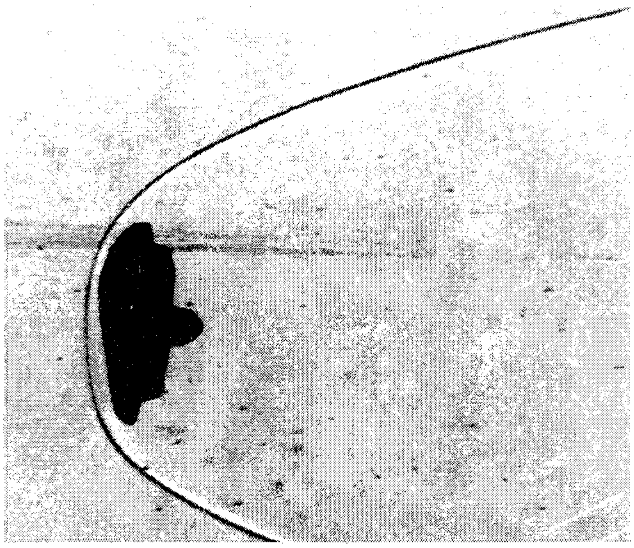

Fig. 5 Shadowgraph showing flowfield structure about simple ASTV model (photograph courtesy of R. Kruse, NASA Ames).

must not have lift at trim conditions. The difficulties of testing in the range and possible solutions will be discussed in more detail in a later section of this paper. Despite the problems, a wide variety of tests have been conducted in aeroballistic ranges including determination of aerodynamic forces and moments, documentation of flowfield structures such as shock shapes, free shear layers and wakes, investigations of boundary layer transition, heat transfer (convective and radiative), and studies of the effects of ablation materials. Typical data obtained at the HFFAF will be described briefly to illustrate some of the tests that have been performed in aeroballistic ranges.

Aerodynamic coefficients are obtained from aeroballistic range data in the following manner. As the model travels in free flight down the test section, model position, orientation, and time-of-flight are recorded on film and chronographs. A data reduction routine then fits the equations of motion to the measured trajectory data by using a least-squares procedure. This method of determining aerodynamic coefficients is unlike techniques used in conventional facilities; however, it is similar to those used to obtain data from flight experiments. A more detailed discussion of these reduction methods can be found in Refs. 7 and 8. The aerodynamic coefficients can be determined to within several percent over a wide range of Mach numbers and angles of attack. The data presented in Fig. 4 are based on data from Ref. 8. The data show the drag and pitching moment coefficients for a blunted 5-deg half-angle cone flying at 5 km/s and at a Reynolds number of 10^6 compared with calculations performed by G. Molvik. A histogram showing the number of data points collected at each angle of attack is also shown. For this data, error estimates indicate that accuracies over the entire angular range are better than 3%. Accurate determination of aerodynamic coefficients at hypervelocity is essential for the design of high-speed flight vehicles, and the aeroballistic range can play an important role in obtaining these coefficients.

Flow structure can be studied by using shadowgraph photos, which are taken at all stations during aeroballistic range launches. Figure 5 shows a typical shadowgraph of an ASTV-like vehicle in flight.[9] The particular point of interest for this test was to determine whether the free shear layer coming from the corner of the model would impinge on the afterbody and cause a region of high heat transfer. Other features shown in this figure are bow and wake shocks as well as the beginning of the wake flow. The range can be used to great advantage in the study of wake flows at high-speed conditions since this region is unobstructed by stings. All of these features can be useful in CFD code verification, and accurate determinations of the

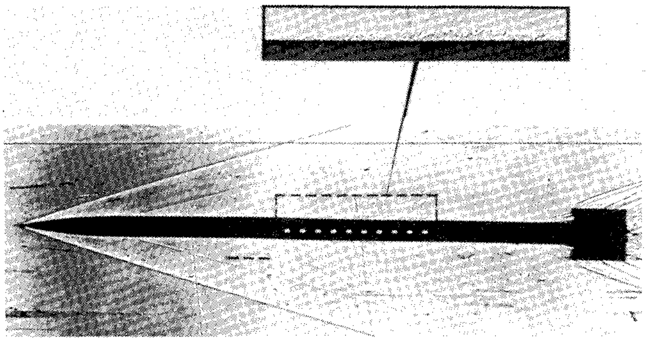

Fig. 6 Shadowgraph showing transition on a pencil model at Mach 3.9.[10]

bow shock standoff distance are good indicators of the chemical state of the shock layer. Range shadowgraphs have also been used to study the transition to turbulence. Figure 6 shows an example of one such study, reported in Ref. 10. The figure shows a shadowgraph of a model flying at a Mach number of 3.9 and a Reynolds number per inch of 2.2×10^6. Evidence of turbulent bursts is clearly seen in the shadowgraph. The "unit Reynolds number effect," which is inferred from tests in conventional wind tunnels, is believed to result from noise generated in the wind tunnel flow. The aeroballistic range provides a much lower ambient noise level; however, the importance of this effect in the range is still unknown.

Convective and radiative heat transfer have also been measured in the aeroballistic range. In one test, the heat transfer was inferred from the time the surface material (aluminum or nickel) started to melt.[11] This method has an accuracy of $\pm 10\%$, which is well within the scatter of available shock tube data. Measurements of emission spectra from the stagnation shock layer formed about blunt aeroballistic range models have been used to deduce radiative properties for both thermochemical equilibrium and nonequilibrium flows.[12,13] Spectra from broadband radiometers were analyzed to predict the equilibrium and nonequilibrium radiative heat transfer to the forebody of the Apollo vehicle. Spatial distributions of shock layer emission also have been measured by nearly head-on observations of aeroballistic range models by employing a calibrated image converter camera or a scanning method which focused light from the shock layer onto a small aperture in front of a photomultiplier tube.[9,14]

A novel technique, called time-of-flight scanning spectrometry,[15-17] has been used to obtain spatially integrated spectra from the radiating shock layer. As the model flies through the focal plane of the collecting mirror, the luminous shock layer acts as a moving entrance slit, sweeping out the spectrum of the shock-heated gas on the exit slit. The spectrally resolved light from the shock layer passes through the exit slit of the spectrometer falling upon a photon sensor, whose output is recorded with an oscilloscope. The spectral resolution is set mainly by the geometry of the shock layer emission, the exit slit width, and the reciprocal dispersion of the spectrometer. An actual record obtained with such a device is shown in the inset in Fig. 7.[17] These data were obtained under nonequilibrium shock layer conditions at a velocity of 6.3 km/s in a gas then thought to be representative of the Martian atmosphere. Similar work could provide CFD calibration data on equilibrium and nonequilibrium shock layer flows in air and other gases of interest, such as CO_2.

Future Aeroballistic Facilities

The flight environment of future missions will stretch the simulation capabilities of existing facilities, and CFD validation needs will require detailed data difficult to obtain in high-enthalpy facilities. The aeroballistic range offers many advantages in the testing of hypersonic vehicles, and many of the questions concerning aerothermodynamic phenomena can be answered in our existing ranges by adapting modern diagnostic techniques. In some cases, proper simulation of the flight environment can only be achieved by launching models at higher speeds or by launching larger models. New gun technology is needed to accomplish this. Some concepts for advanced instrumentation and improved launch capabilities are discussed below.

Instrumentation

Obtaining high quality data is a continuing problem for researchers in the aeroballistic range, and many ingenious techniques have been used to obtain quality data in this difficult environment. To date most diagnostics employed in the range have been, of necessity, optical. Because the models are relatively small and the position of the model as it passes a measurement station cannot be predicted precisely, spatial resolution is sacrificed to insure that the model is captured in the optics. The uncertainty in the position of the model can be minimized by guiding it within a set of tracks, as is done at AEDC,[18] but this rules out aerodynamic force and moment determinations. The speed with which the model passes the measurement station dictates submicrosecond exposure times to eliminate the effects of motion blur, and extremely powerful light sources, faster optics, and more sensitive sensors are required. Current advances in lasers, optics, and computational capability, generally, have not been employed in the aeroballistic range because of the past reduced interest in hypervelocity phenomena. In the following paragraphs, some of these advances will be mentioned as possible candidates for range instrumentation.

The accuracy to which aerodynamic coefficients can be determined is dependent on the accuracy to which the model position, orientation, and time-of-flight can be measured, the amount of free-flight motion experienced by the model, and the precision to which data-reduction routines can match the measured trajectory. Advances in image processing and electronics offer the possibility of improving the accuracy to which the position, orientation, and time-of-flight of models can be measured. Also improvements have been made in the last several years in available data-reduction routines. Modern routines are capable of reducing data from multiple tests simultaneously and yielding the nonlinear effects of angle of attack and velocity change on aerodynamic coefficients directly.[7,8,19] Work is proceeding to extend these routines to determine aerodynamic coefficients for nonaxisymmetric models and for models which exhibit hysteresis in aerodynamic coefficients.

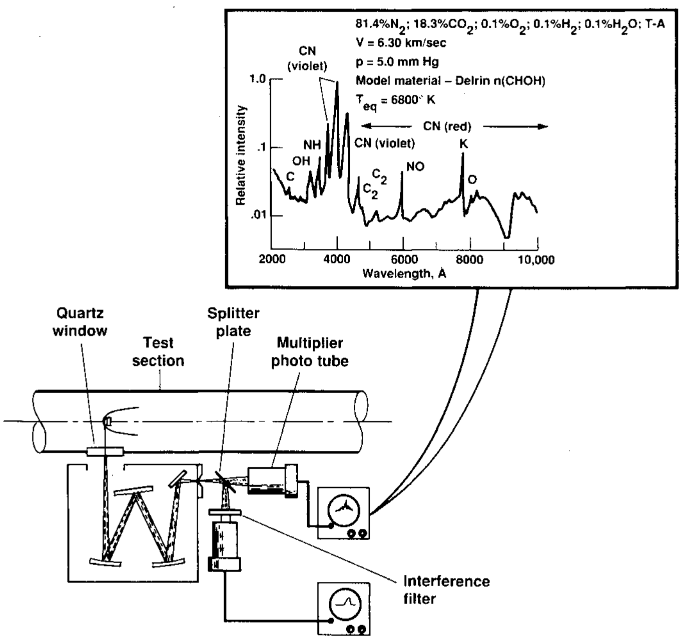

Fig. 7 Typical data obtained from a free-flight aeroballistic range test using a time-of-flight scanning spectrometer.[16,17]

Flowfield structure data are typically obtained from shadowgraphs, but schlieren and holographic interferometry systems are sometimes used.[20-22] All of these systems lose sensitivity at low densities where chemical-kinetic effects are most important, and efforts are underway to increase the sensitivity of the Ames interferometer.

Studies of transition to turbulence can be made in the range using shadowgraphs and infrared (IR) photography, but several factors must be considered. The surface roughness of the model must be known accurately. Direct incident-light photographs of the model in flight should be made in order to determine if the model has suffered any damage during launch and to see if there is any evidence of ablation affecting the transition to turbulence. Freestream turbulence levels must be measured to characterize the unit Reynolds number effect. The temperature of the model surface is important and should be measured. From the distribution of temperatures on the model surface, the heating history and location of spatially stable boundary layer transition can be inferred. Sudden increases in the surface temperature gradient along a streamline can indicate the onset of transition.

Presently, model surface temperatures can be measured by observing the visible and IR emission from the model surface material. In such a system at AEDC,[14] spatial resolution of 0.3 to 1.5 mm and temporal resolution of about 100 ns have been achieved by frontal-imaging of a bluff body. Temperatures in a range of 1200 to 5000 K can be measured to an accuracy of about ±150 K. But resolution on the planform of the model continues to be a problem, especially in the IR where sensors are not fast. Advances in sensor technology will help in this area; however, the major source of error in these systems is determination of the emissivity of the model material. Emissivity is a function of the temperature of the surface, the condition of the surface, and the heating history of the surface. A possible alternative to the IR techniques is the use of thermographic phosphors. These have been developed for temperature measurement of engine parts[23] and do not depend on the emissivity of the material. With this technique it will be possible to measure surface temperatures faster and more accurately than with present systems.

Because the model passes by the measurement station so rapidly, usually only one measurement can be made at any one station with a given instrument. For this reason, measurement schemes which obtain data in two or three dimensions, such as planar laser-induced fluorescence and tomographic techniques, should be emphasized in the aeroballistic range. Obtaining two-dimensional images of the velocity, density, temperature, and species in the flow are important, especially in the validation of CFD codes. Nonintrusive techniques have been devised to measure these quantities by use of laser absorption and laser-induced fluorescence.[20,24-28] Many of these techniques obtain two-dimensional information by imaging onto CCD arrays or image-intensified cameras. The low number densities characteristic of the hypervelocity regime, however, result in a low signal to noise ratio, and this problem must be addressed. Additionally, advances in imaging technology can be used to improve many of the techniques that have been used in the range, for instance the measurement of radiative heat transfer and emission spectra.

Onboard instrumentation can be very useful in measuring surface temperature, heat transfer, and pressure. Such measurements can serve as independent corroboration for measurements made with other instruments or provide a single absolute value to calibrate techniques that provide only relative information. The small size of present range models restricts the number and sophistication of instruments that can be carried onboard. Also, the high acceleration loads experienced during launch provide severe restriction on the kinds of instruments that can be carried aboard the model. Previous systems employed ratio transmitters to telemeter information from onboard sensors. At speeds in excess of 4 km/s, however, the shock wave in front of the model ionizes the air creating interference with the radio signal. A project underway at Ames is exploring the use of IR laser diodes to telemeter information from onboard sensors.[20]

Launch Options

Concerns about spatial resolution in optical diagnostics and the need to put instrumentation onboard the model tend to drive model sizes larger. But these problems can also be solved by improvements in optical diagnostics or by further miniaturizing electronics. There is another, more important, reason for seeking larger model sizes. That is the question of correctly scaling the chemical kinetics. In order to obtain the proper chemical kinetics, the correct enthalpy is required (by matching velocity) and the collision frequency between molecular and atomic species must match those experienced in flight. In compression regions, such as the stagnation region of a blunt body, where dissociation occurs, two-body collisions dominate the kinetics. This requires that the product of density and length scale, ρL, be matched. In a region where recombination occurs, such as the expansion in a nozzle or around a corner, three-body collisions play an important role in the kinetics. Matching the three-body collisions accurately requires that $\rho^2 L$ be matched. Since questions of appropriate scale plague all ground-based facilities, it may not be possible to achieve the proper chemical scaling in anything but a full-scale flight vehicle. For the purposes of CFD code validation, however, it is not important that both be matched exactly. It is important that the test be carried out under conditions where both two- and three-body collisions are important in order to test the chemistry in the code. Thus ground-based facilities can be used to verify the CFD codes that will be used to design full-scale flight vehicles. Studies involving nonequilbrium phenomena can be investigated in shock tubes and shock tunnels, but these classes of facilities suffer from spatial and temporal nonuniformities, and the effect of freestream contaminants on nonequilibrium phenomena has not yet been established. Use of the aeroballistic range mitigates these effects, and actual flight enthalpies can be attained. In order to properly study nonequilibrium phenomena, experiments in a variety of facilities and flight experiments need to be conducted together with computational modeling. Questions of model scale plague all ground-based facilities. This motivates the effort to increase the model size and hence the launch mass capability of aeroballistic ranges.

The most common model launchers for high-performance aeroballistic ranges at present are two-stage light-gas guns. The requirement to launch larger models at higher speeds dictates an improvement of the present launching capabilities of these guns. In this section, the operation and performance of the light-gas gun will be reviewed and potential increases in performance discussed. Several new technologies that, theoretically, offer considerable increases in performance over the light-gas gun are under development. The strengths and status of the most promising of these new technolgies, namely the rail gun and "ramjet-in-tube," will be reviewed in this section.

The two-stage light-gas gun is the product of rapid development during the 1960s. The gun uses a charge of smokeless gunpowder to accelerate a heavy piston to a moderate velocity (less than 1 km/s) down the pump tube. The piston in turn compresses a charge of propellant gas, usually hydrogen, to several kilobars pressure. Upon release by a burst diaphragm, the charge gas propels the model to high speed in the launch tube. This system provides a wide selection of operating conditions and permits the launch of a wide range of model mass with acceptable peak acceleration and jerk (the derivative of acceleration with respect to time). The chief drawbacks of the present technology are the small size of the model (presently less than 6 cm in diam or 800 kg in mass), the high peak accelerations (on the order of 150,000 to 500,000 g) and the maximum launch velocity (normally less than 10 km/s).

During the last 30 years, much effort has been expended in attempting to launch small projectiles to hypervelocities using rail guns (see for example Ref. 29). A pair of rails, on opposite sides of the launch tube, complete an electrical circuit when an armature conductor connects them. The remaining surfaces, which complete the bore, are insulators. When a current is forced to flow along one rail through the armature (metal or plasma at the base of the projectile) to the opposite rail and back to the power supply, the projectile is propelled by the resulting $J \times B$ force. As the projectile moves, the increasing resistive losses in the rails and diminishing energy in the supply source make it necessary to disconnect the initial source and to connect the next supply source. The rail gun offers the advantage that launch accelerations can be tailored to the application at hand and high projectile speeds are possible in principle. The performance of the rail gun at present appears to be limited to launching projectile masses of a few grams to speeds of 4–15 km/s.[30] One major difficulty preventing improvement of rail gun performance is confinement of the plasma armature. The strong repulsive forces between the rails tend to open a gap between the projectile and rail allowing plasma to escape. This plasma must be replenished by vaporizing material from the rails, which results in severe rail erosion. The problems of rail erosion and high loading (leading to plasma escape) may prevent the rail gun from competing with the two-stage light-gas gun in the near future.

The ramjet-in-tube concept[30] has been developed recently. In this concept, a finned projectile travels down a tube filled with a combustible gas mixture. The projectile acts as the ramjet centerbody, and the tube wall acts as the ramjet cowl. In the thermally choked subsonic combustion mode, a normal shock stands on the projectile, aft of the throat, and the flat base of the projectile acts as a flame-holding dump combustor. This mode of operation has been experimentally demonstrated from velocities of 0.7 to 2.3 km/s. Relatively constant accelerations of about 20,000 g have been achieved with a 50-g, 38-mm projectile. Calculations indicate that a drive mode using oblique detonation waves should operate effectively up to velocities of 7 to 10 km/s, and the concept is being studied at the University of Washington.[31] The ramjet-in-tube concept offers relatively constant accelerations and can be scaled from projectile masses of grams to thousands of kilograms. Considerable development work must still be done before the ramjet-in-tube concept can be used in the aeroballistic range.

In the near term, therefore, increases in model size seem likely only through enlargement of the light-gas gun. Experience has shown that light-gas gun technology scales favorably with launch tube diameter, and it is reasonable to assume that a 25-cm-diam launch tube can be designed to launch projectiles of about 30 kg to 8 km/s. The acceleration loads experienced by models during launch diminish as the gun is scaled up in size. A fundamental limitation on the present light-gas gun design is that all of the launch energy must be applied at the launch-tube breech; no workable scheme has been developed to permit staging of the guns in a manner contemplated for electromagnetic guns or the ramjet-in-tube. It is expected, however, that coupling an electromagnetic rail or ramjet-in-tube to the muzzle of a light-gas gun might permit each to operate in its optimal speed range. The electromagnetic rail gun works best at high speed because the load-dwell time at any point is short, which minimizes damage to the rails. The ramjet-in-tube operating in the detonation mode requires that the projectile enter the tube at a certain minimum velocity that will support detonation of the fuel-air mixture. Developmental work is needed before a launch system composed of more than one technology can be employed in an aeroballistic range.

Conclusions

Future missions will require a better understanding of the aerothermodynamics of hypervelocity flight. Because many future missions will fly in regimes outside of the simulation capability of present ground-based facilities, CFD will be used increasingly in the design of these mission vehicles. Our ground-based facilities will be used extensively to develop a better understanding of the underlying physical phenomena involved and in calibrating the CFD codes used in vehicle design. The aeroballistic range is a very useful facility for such hypervelocity testing. It is capable of excellent Mach number and enthalpy simulation over a wide range of conditions, has a very clean freestream chemistry, and has small freestream disturbances. At present, the models must be relatively small and simple, and data acquisition can be difficult. By employing advanced diagnostics and developing the ability for onboard instrumentation, some of the questions concerning aerothermodynamic phenomena can be answered in our present facilities.

Mission requirements and the need for onboard instrumentation require the development of guns that can launch larger projectiles to higher velocities than are presently attainable with light-gas guns. The operation and status of the main launching alternatives have been presented; however, at present, none of these have reached the stage in their development to be considered as replacements for the two-stage light-gas gun. For the near term, it appears that enlargement of the light-gas gun will result in some increase in model size. At AEDC, a light-gas gun with a 10-cm-diam launch tube is being designed. This gun should be able to launch a mass of about 3 kg to about 7.5 km/s. NASA Ames has proposed a study which would couple a ramjet-in-tube to a light-gas gun to demonstrate the feasibility of this concept. NASA Langley has proposed the construction of a large-scale (25–40-cm-diam launch tube) aeroballistic range, which would employ both light-gas gun and rail gun technology. It seems advisable to concentrate an effort in the development of advanced instrumentation to enhance the capabilities of the existing ranges. This increased diagnostic capability will also be needed in a large-scale aeroballistic range.

References

[1]National Commission on Space, *Pioneering the Space Frontier*, Bantam, New York, 1986.

[2]"National Aeronautical R&D Goals—Agenda for Achievement," Executive Office of the President, Office of Science and Technology Policy, Washington, DC, 1987.

[3]Walberg, G. D., "A Survey of Aeroassisted Orbital Transfer," *Journal of Spacecraft and Rockets*, Vol. 22, No. 1, 1985.

[4]Jones, J. J., "The Rationale for an Aeroassisted Flight Experiment," AIAA Paper 87-1508, June 1986.

[5]William, R. M., "National Aero-Space Plane: Technology for America's Future," *Aerospace America*, Nov. 1986.

[6]Canning, T. N., Seiff, A., and James, C. S., "Ballistic Range Technology," AGARD 138.

[7]Whyte, R. H., Winchenbach, G. L., and Hathaway, W. H., "Subsonic Free-Flight Data for a Complex Asymmetric Missle," *Journal of Guidance and Control*, Vol. 4, No. 1, 1981, p. 59.

[8]Strawa, A. W., Molvik, G., Yates, L. A., and Cornelison, C., "Experimental and Computational Results for 5 Degree Blunt Cones with Shock Generators at High Velocity," AIAA Paper 89-3377, Aug. 1989.

[9]Intieri, P. F., and Kirk, D. B., "High-speed Aerodynamics of Several Blunt-Cone Configurations," *Journal of Spacecraft and Rockets*, Vol. 24, No. 2, 1987, pp. 127–132.

[10]James, C. S., "Observations of Turbulent-Burst Geometry and Growth in Supersonic Flow," NACA TN-4235, 1958.

[11]Compton, D. L., and Cooper, D. M., "Free-Flight Measurement of Stagnation-Point Convective Heat Transfer at Velocities to 41,000 ft/sec," NASA TN-D-2871, June 1965.

[12]Craig, R. G., and Davy, W. C., "Absolute Radiometers for Use in Ballistic-Range and Shock-tube Experiments," NASA TN-D-5360, Oct. 1969.

[13]Page, W. A., and Arnold, J. O., "Shock Layer Radiation of Blunt Bodies at Reentry Velocities," NASA TR-R-193, 1964.

[14]Hendrix, R. E., and Dugger, P. H., "Role of High Speed Photography in the Testing Capabilities of the Arnold Engineering Development Center (AEDC) Range and Track Facilities," *Proceedings of the 15th International Congress on High Speed Photography and Photonics*, San Diego, CA, Aug. 1982.

[15]St. Pierre, C., "The Visible Emissions from 0.5 inch Hypervelocity Models Measured with a Moving Target Scanning Monochroma-

tor," CARDE TM AB-59, 1960.

[16]Reis, V. H., "Oscillator Strengths for the N2 Second Positive and N2+ First Negative Systems from Observations of Shock Layers about Hypersonic Projectiles," *Journal of Quantitative Spectroscopy and Radiant Transfer*, Vol. 4, pp. 783-792.

[17]Whiting, E. E., "Determination of Mars Atmospheric Composition by Shock-Layer Radiometry During a Probe Experiment," AIAA Thermophys. Spec. Conf., New Orleans, April 1967.

[18]Air Force Systems Command, "AEDC Test Facilities Handbook," U.S. Air Force, Arnold Engineering Development Center, TN, March 1984.

[19]Winchenbach, G. L., Uselton, R. L., Hathaway, W. H., and Chelekis, R. M., "Free-Flight and Wind-Tunnel Data for a Generic Fighter Configuration," *Journal of Aircraft*, Vol. 21, No. 1, 1984, pp. 5-13.

[20]Butler, G., Nguyen, B., King, D., and Abate, G., "Ballistic Range Flowfield Measurements of the Hypervelocity Near Wake of Generic Shapes and Correlation with CFD Simulation," AIAA Paper 90-0621, Jan. 1990.

[21]Strawa, A. W., and Cavolowsky, J. A., "Development of Non-Intrusive Instrumentation for NASA-Ames' Ballistic Range and Shock Tunnel," AIAA Paper 90-0628, Jan. 1990.

[22]Sharma, S. C., and Park, C., "A Survey of Simulation and Diagnostic Techniques for Hypersonic Nonequilibrium Flows," AIAA Paper 87-0406, 1987.

[23]Noel, B. W., et al., "Evaluating and Testing Thermographic Phosphors for Turbine-Engine Temperature Measurement," AIAA Paper 87-1761, 1987.

[24]Kychakoff, G., Howe, R. D., and Hanson, R. K., "Quantitative Flow Visualization Technique for Measurements in Combustion Gases," *Applied Optics*, Vol. 23, No. 5, 1984, pp. 704-712.

[25]Cattolica, R., and Vosen, S., "Combustion-Torch Ignition: Fluorescence Imaging of OH Concentration," *Combustion and Flame*, Vol. 68, No. 3, 1987, pp. 267-281.

[26]Miles, R. B., Connors, J. J., Howard, P. J., Markovitz, E. C., and Roth, G. J., "Proposed Single-Pulse Two-Dimensional Temperature and Density Measurements of Oxygen and Air," *Optics Letters*, Vol. 13, March 1988, pp. 195-198.

[27]Chang, A. Y., Rea, E. C., and Hanson, R. K., "Temperature Measurements in Shock Tubes Using a Laser-Based Absorption Technique," *Applied Optics*, Vol. 26, No. 5, 1987, pp. 885-891.

[28]Gross, K. P., McKenzie, R. L., and Logan, P., "Measurements of Temperature, Density, Pressure, and Their Fluctuations in Supersonic Turbulence Using Laser-Induced Fluorescence," *Experiments in Fluids*, Vol. 5, 1987, pp. 372-380.

[29]Haight, C. H., and Tower, M. M., "Distributed Energy Store (DES) Railgun Development," *IEEE Transactions on Magnetics*, Vol. Mag-22, No. 6, 1986.

[30]Hawke, R. S., Nellis, W. J., Newman, G. H., Rego, J., and Susoeff, A. R., "Summary of EM Launcher Experiments Performed at LLNL," *IEEE Transactions on Magnetics*, Vol. Mag-22, No. 6, 1986.

[31]Hertzberg, A., Bruckner, A. P., and Bogdanoff, D. W., "The Ram Accelerator: A New Chemical Method for Accelerating Projectiles to Ultrahigh Velocities," *AIAA Journal* (to be published).

[32]Kull, A. E., Bumham, E. A., Knowlen, C., Bruckner, A. P., and Hertzberg, A., "Experimental Studies of Superdetonative Ram Accelerator Modes," AIAA Paper 89-2632, July 1989.